Eur. Phys. J. Special Topics **225**, 715–728 (2016)

DOI: 10.1140/epjst/e2016-60013-9

THE EUROPEAN PHYSICAL JOURNAL SPECIAL TOPICS

Review

Surface structuring of particle laden drops using electric fields

P. Dommersnes[a] and J.O. Fossum[b]

Department of Physics, Norwegian University of Science and Technology – NTNU, Trondheim, Norway

Received 26 January 2016 / Received in final form 25 May 2016
Published online 15 July 2016

Abstract. Emulsion drops readily adsorb particles at their surfaces, which may lead to a fluid or solid layer encapsulating the drop, known as an armored drop. In this review, we discuss how electric fields can be used to manipulate colloidal surface structures, by dielectrophoretic or electro-hydrodynamic mechanisms and we also compare this to related phenomena in lipid bilayer vesicles. The phenomena discussed are important for a wide range of uses of particle laden drops, including emulsion stabilization, Janus or patchy mesocapsule-, scaffold- or other materials-production.

1 Introduction

Particle laden drops (or Pickering [1] drops), are used for emulsion stabilization (Pickering emulsions [2–4]), and may be used in material production [5,6]. A particle laden Pickering drop can be produced by microfluidic methods [7] or by applying electric fields [8,9], and the particles can be sintered or linked to form rigid capsules, called colloidosomes [10,11].

Electric field manipulation of particles on drop interfaces includes mechanisms based on dielectrophoresis [12], electro-hydrodynamics [13], and drop electrocoalescence[14]. It has been observed that dielectrophoretic structuring of particle laden drops exposed to an external uniform electric field, can occur in two different ways: (i) Via dielectrophoretic transport of particles in the non-uniform electric field at the drop surface, in which case the dipole of the particle interacts with the field gradients at the drop surface, resulting in transport of particles either to the "drops electric poles", or to the "drops electric equator", or: (ii) Via dielectrophoretic interactions between the particles themselves, i.e. dipole-dipole interactions leading to electrorheological chain formation [15,16] confined to the drop surface. Such effects can be used for separating two types of particles at the surface of a drop [17], or for removal of particles from drop surfaces, [18] as well as for destabilization of Pickering emulsions using external electric fields [19].

[a] e-mail: paul.dommersnes@ntnu.no
[b] e-mail: jon.fossum@ntnu.no

One essential factor for particle structuring at drop interfaces is the capillary binding mechanisms, i.e. that the binding energy of any particle at a liquid-liquid interface is proportional to the product of the surface tension between the two liquids and the particle surface area [20]. For micro meter sized particles this binding energy is order of magnitude 10000 kT, which means that colloidal particles in general are very strongly bound to liquid-liquid interfaces.

The particle flow patterns introduced above are caused by two different kind of electric field induced mechanisms, dielectrophoretic, or electro-hydrodynamic, in AC or DC electric fields. Similar flow patterns have been observed in lipid vesicles in AC electric fields [21].

In this review we will first discuss particle structuring on single drops by dielectrophoretic mechanisms, and then compare this to cases where electro-hydrodynamics is the governing mechanism. We will then review situations for two interacting drops, or two interacting vesicles and point to the potential that such fusion phenomena may offer for production of advanced meso-/nano-shells, colloidosomes or particles, including Janus [22] or patchy [23] entities. Finally we will discuss some emerging directions in this area.

2 Particle structuring on drops by dielectrophoresis

There are essentially two mechanisms for dielectric induced ordering of particles at drop interfaces: One is a single-particle effect that is driven by the inhomogeneous electric field at the drop interface where particles are attracted to the extrema of the electric field (i.e. the drop electric poles or equator). The other mechanism is due to dielectrophoretic interactions between the particles (electro-rheology).

Nudurupati et al. [12] applied a uniform AC electric field in order to change the distribution of particles on the surface of a drop immersed in another immiscible carrying liquid, thus obtaining well-defined concentrated regions at a drop surface while leaving the rest of the surface free from particles. This in part depends on the so-called Clausius-Mossotti (C-M) factor, which sign is given by the difference between the polarizabilities of the media (particles or liquids). Nudurupati et al. [12] studied a system for which the dielectric constant of the drop liquid is smaller than that of the carrying liquid, in which case the electric field magnitude is largest at the electric equator, and the particles with a positive (C-M) factor move along the drop surface to the equator, as is displayed in Fig. 1. In contrast, particles with a negative C-M factor will move towards the drop electric poles. The opposite takes place when the dielectric constant of the drop liquid is larger than that of the carrying liquid in which case the electric field magnitude is largest at the drop poles, and the particles with a positive C-M factor migrate towards the poles, while those with a negative C-M factor move to form a ring at the drop equator [12]. It is worth noticing that this dielectrophoretic force scales like the volume of the particle, thus the dielectrophoretic structuring mechanism is less efficient for smaller particles.

In Fig. 2, the polarized polymer particles form dipolar chain aggregates parallel to the applied AC electric field, including chain bundling, which is also commonly observed in bulk electrorheological systems [25]. Figure 3 shows a different case, where conducting metallic particles subject to a DC electric field, confined to a drop surface form dipolar chains similar to Fig. 2, but in this case the chains repel one another rather than bundle together. The mechanisms for ribbon formation at the electric equator are different between Fig. 2 (dielectrophoretic motion of the particle in the inhomogeneous electric field at the drop surface) and Fig. 3 (Taylor electro-hydrodynamics plus dielectrophoretic dipolar chain formation). It is not understood whether this is related to the hitherto unresolved question about why some chain

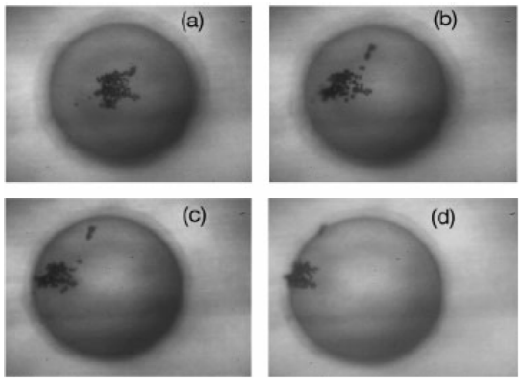

Fig. 1. The pictures show the top view of the motion of hollow 18 micrometer diameter glass spheres on the surface of a silicone oil drop suspended in corn oil and subjected to a uniform AC electric field pointing normal to the plane of the picture. The drop diameter was approximately 0.7 mm, and the applied field approximately 830 V/mm. The Clausius–Mossotti (C-M) factor of the particles is positive, as described in the text, and the particle assembly migrates towards the electric equator, where the electric field magnitude is maximal. The time evolution (a)–(d) is 600 s. The picture is taken from Nudurupati et al. [12].

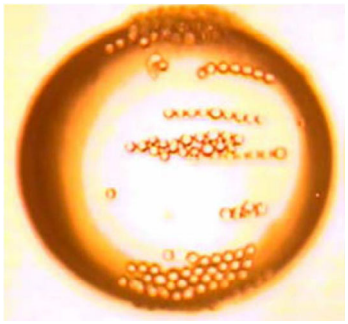

Fig. 2. Example of dielectrophoretic concentration of particles at the electric equator of a silicone oil drop embedded in castor oil. The picture is taken from Nudurupati et al. [24], and displays the distribution of 70 micrometer diameter polymer spheres on the surface of a 1.6 mm diameter silicon drop, subjected to a horizontal uniform AC electric field, which means that the active mechanism at work is dielectrophoresis, and not Taylor electrohydrodynamics as it would be in a DC field, see Fig. 3. It is seen that the particles become polarized in the AC field forming dipolar electrorheological chains parallel to the electric field, followed by chain migration towards the drop electric equator by dielectrophoresis, like in Fig. 1, and subsequent aggregation of chains into bundles.

systems confined to drop interfaces bundle (Fig. 2) like in bulk systems, and why some chain systems do not bundle (Fig. 3).

The dielectrophoretic effects combined with dipolar particle aggregation, such as those discussed above are active for particles that can be polarized sufficiently for the induced dipolar forces to dominate over other forces such as gravitational or hydrodynamic forces. This means that the particles must have low enough mass for gravitational effects to be non-dominant, and the particles must have a sufficient size in order to carry a large enough induced dielectric- or conductivity-based dipole for the electrophoretic and dipolar effects to be practically active. The dielectrophoretic force on the particles [12] scales like the volume of the particle, as noted above. In contrast, the hydrodynamic Stokes force acting on a particle scales as its radius, and

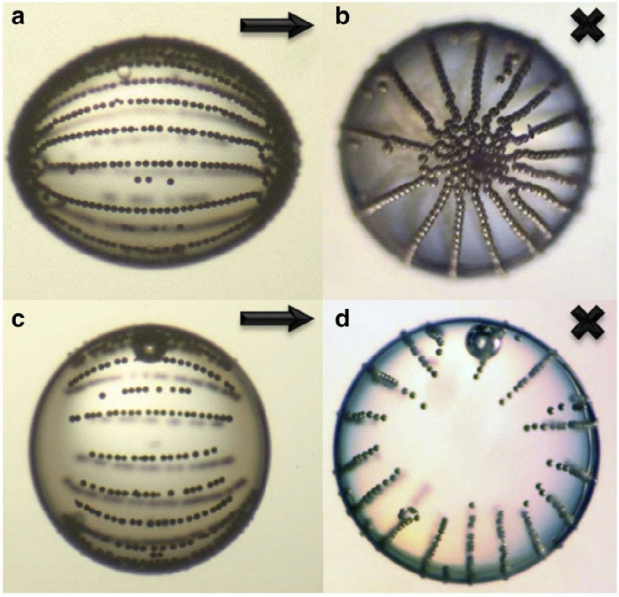

Fig. 3. Dipolar electrorheological chain formation of conducting metallic particles for two different particle concentrations (a,b) and (c,d), confined to the interface of a silicon oil drop suspended in castor oil. In contrast to the case in Fig. 2, the chains here are equidistant (i.e. no bundling). The picture is taken from Dommersnes et al. [8]. The drop size is approximately 2 mm. The arrows and crosses indicate the direction of the DC electric field.

will dominate over the dielectrophoretic force for small enough particles, under which condition hydrodynamic forces may dominate the particle structuring.

3 Particle structuring by electro-hydrodynamics

The field of electro-hydrodynamics was initiated by G.I. Taylor in his seminal paper from 1966 [26], where he presented a model supported by experiments, explaining the observations previously made by Alan and Mason [27] that drops exposed to a uniform DC electric field sometimes deform and elongates perpendicular to the applied electric field (termed oblate deformation), rather than along the electric field axis (termed prolate deformation), as is expected for regular non-conducting purely dielectric liquids. G.I. Taylor's insight was that for liquids with a finite electric conductivity, specifically for so-called leaky dielectrics, there is conductivity induced free charge build-up on drop interfaces, which is additional to the dielectrically induced charges, and that these extra charges give rise to local electric stresses on the drop interface. These stresses will in turn induce hydrodynamic flows inside and outside the liquid drop, and also induce an oblate deformation. The time scale for the charge build-up is determined by the Maxwell-Wagner charge relaxation time, which is given by the ratio of the mediums dielectric constant and its electric conductivity [28]. In AC electric fields at sufficiently high frequencies much larger than the inverse Maxwell-Wagner relaxation time, electro-hydrodynamic flow is not active.

Figure 4 shows calculated and experimentally observed electro-hydrodynamic flow patterns and oblate deformation of a silicone oil drop embedded in a castor oil bath. The direction of the observed flow patterns form the poles to the equator in this

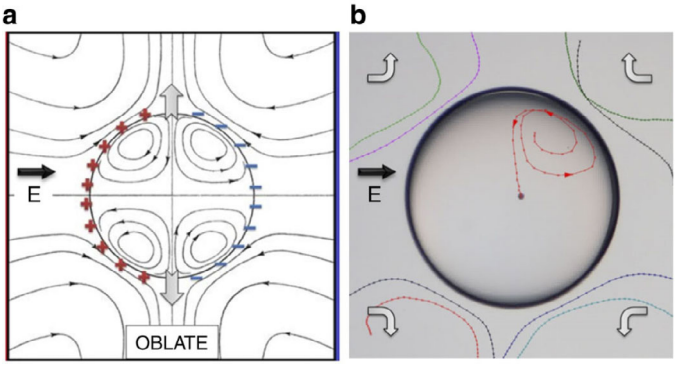

Fig. 4. Hydrodynamic streamlines in Taylors electro-hydrodynamic drop model. The Figure is taken from Dommersnes et al. [8]: (a) is adopted from Taylor's original paper [26]. (b) Which was measured experimentally by Dommersnes et al. [8] is displaying trace paths from poly-ethylene beads around the drop, and one bead inside. The drop diameter is approximately 2 mm. The arrows indicate the directions of the stream lines. The DC electric field direction is horizontal in the plane of the panels, as indicated by the arrows.

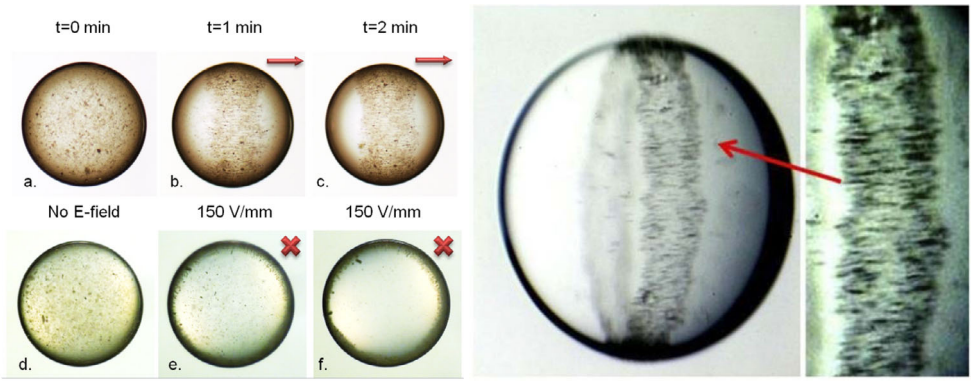

Fig. 5. The panels taken from Dommersnes et al. [8] display electro-hydrodynamic assembly of colloidal clay surface ribbons. (a)–(f) Are perspective views at different times of the same 0.7 mm diameter silicone drop embedded in a castor oil bath, exposed to a uniform DC electric field with direction as indicated in panels. Before the electric field was switched on, i.e. (a) and (d), the clay particles were evenly distributed inside the drop. Electro-hydrodynamic circulation flows are observed in the drop immediately after the electric field is turned on, and in a few minutes the clay particles are concentrated in a ribbon-shaped film near the electric equator on the drop surface. The right panel is a close-up showing quasi two-dimensional electrorheological dipolar chain formation of clay particles within the ribbon. The DC electric field strength was 200 V/mm.

case are due to the longer Maxwell-Wagner charge relaxation time of the silicon oil compared to the castor oil.

Figure 5 displays the same kind of situation as in Fig. 4 with larger number of capillary bound particles to the drop interface. In this case the particles, originally evenly distributed inside the silicon oil drop, are driven towards the drop electric equator by Taylor electro-hydrodynamic flow.

In Fig. 4 and Fig. 5 the conductivity ratio between the drop liquid and the embedding liquid is about 1/10, and thus the ratio of the charge relaxation times of the

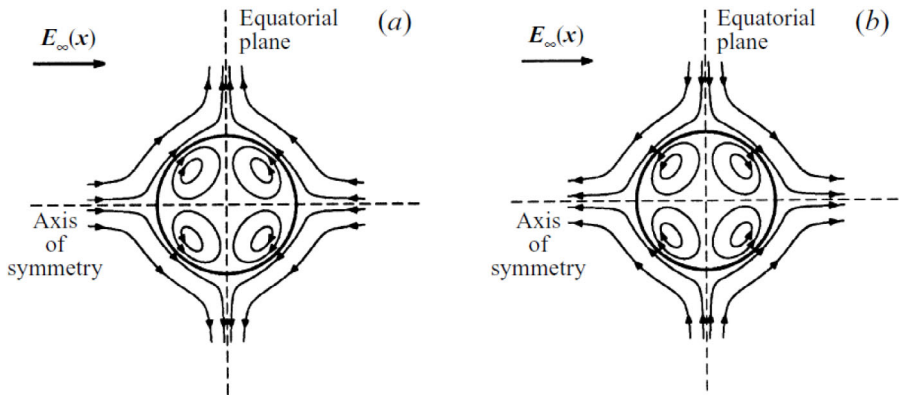

Fig. 6. The sketches which are taken from Baygents et al. [29] illustrate the electro-hydrodynamic flow patterns for the two leaky dielectric cases: (a) The charge relaxation time of the drop liquid is larger than that of the carrying liquid, thus the electro-hydrodynamic flow is directed towards the drop equator and will bring particles there. (b) The charge relaxation time of the drop liquid is smaller than that of the carrying liquid, thus the electro-hydrodynamic stream lines point towards the drop poles and will bring particles there instead.

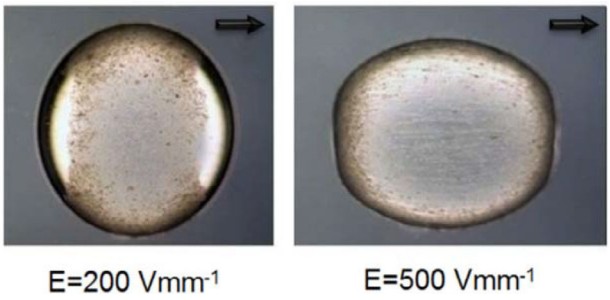

Fig. 7. The pictures taken from Dommersnes et al. [8] display how a drop with a clay ribbon deforms from oblate to prolate shape due to increased DC electric field strength. The ribbon and the associated oblate drop shape formed by electro-hydrodynamic flow carrying clay particles to the drop electric equator at a constant DC electric field strength of 200 V/mm. Subsequently the DC electric field was increased to 500 V/mm, thus increasing the induced electric dipole moment of each clay particle, causing electrorheological chain formation by dielectrophoresis, associated with prolate drop shape along the electric field direction. The original drop radius in this case was about 1 mm. The DC electric field direction was horizontal in the plane of the panels, as indicated by the arrows.

drop and the embedding liquid is larger than 1. In this case the particles are carried by the electro-hydrodynamic flow towards the drop electric equator. If this ratio of the charge relaxation times is smaller than 1, the flow direction is reversed, and the particles should be carried towards the drop electric poles instead, as displayed in Fig. 6.

4 Combined electro-hydrodynamics and dielectrophoresis

Above we have discussed that electric field induced particle assembly by ribbon formation at a drop equator, or alternatively particle assembly at drop electric poles

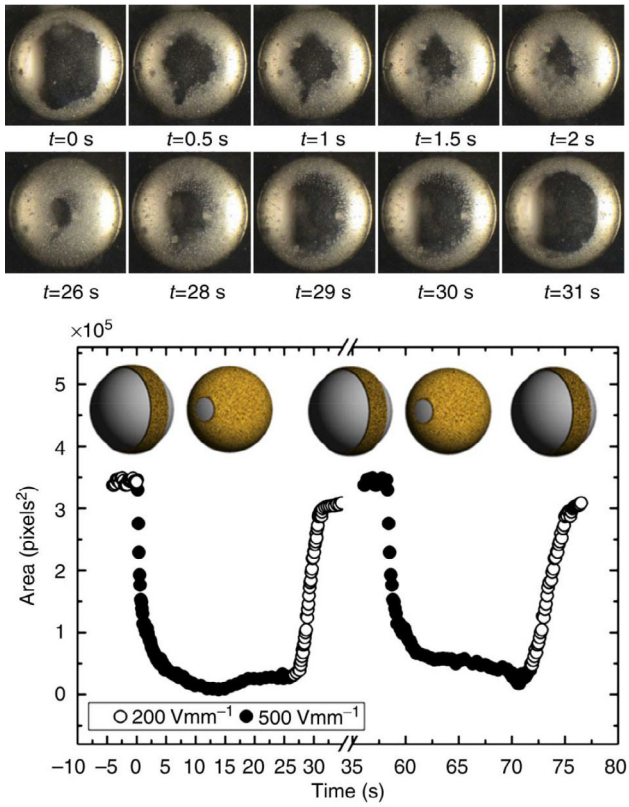

Fig. 8. The panels that are taken from Dommersnes et al. [8] display an actively contracting and expanding pupil armor: This is shown in the series of ten images on the top, where the drop is viewed along the electric field direction (uniform DC electric field). At 200 V/mm, the drop (radius about 1 mm) is partially covered by a clay ribbon, and at 500 V/mm the drop is nearly fully covered by electrorheological dipolar chains confined to the drop interface by capillary forces. The timescale of switching is order of magnitude seconds. This is a reversible process as displayed in the bottom panel, where the area of the pupil opening versus time is plotted, following changes of the electric field strength. The cartoons in the inset display a perspective view of the process.

can be due to two basic mechanisms, the first one from dielectrophoresis, the second one from electro-hydrodynamics. In the former case, the essential materials control parameter is the Clausius-Mossotti factor (its sign and magnitude) which is a purely dielectric parameter at sufficiently high frequency AC electric fields, whereas in the latter case the essential materials control parameter is the conductivity ratio between the liquids, i.e. in this case the effects of finite conductivities of the liquids will dominate over dielectric mechanisms. In certain cases both electro-hydrodynamic effects and dielectrophoretic effects may be present in the same drop system at different applied electric field strengths. Figure 7 and Fig. 8 show examples of this.

5 Vesicle electro-hydrodynamics

Above we have discussed particle flow patterns caused by two different kind of electric field induced mechanisms, dielectrophoretic, or electro-hydrodynamic.

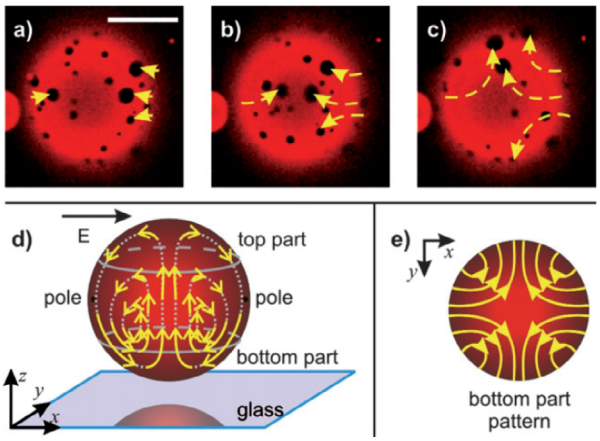

Fig. 9. The panels are taken from Dimova et al. [21], and show electro-hydrodynamic flow in a lipid vesicle. Panels (a)–(c) are confocal micrographs illustrating membrane flow on the bottom part of a lipid vesicle, near the electrode, induced by an AC electric field of magnitude 3.6 kV/mm and a frequency of 80 kHz. The external and internal conductivities are 25 mS/m and 0.3 mS/m, respectively. The time between the consecutive snapshots is approximately 1.3 s. The scale bar is about 50 micrometers. In (d) and (e), the vesicle top and bottom parts, the electric poles and the field direction are indicated, as well as the side (d) and the bottom (e) views of the flow lines.

Similar flow patterns have been observed in lipid vesicles, albeit with important differences: One being that inhomogeneous AC electric fields associated with the proximity of an electrode are needed, the other that the vesicles carry a charge (zeta potential) because they are in water. Vesicles as model systems for biological membranes, and their response to AC or pulsed DC electric fields are important for a number of applications [30]. In uniform AC or DC electric fields the tangential electric stress on a lipid vesicle is balanced by the membrane stretching elasticity (tension). In the vicinity of an electrode, circulation flows in the lipid membrane and in the vesicles have been observed [21] as shown in Fig. 9. It has been shown that a vesicle in an external AC electric field close to an electrode distorts the charge polarization layer near to the electrode, which in turn gives rise to electro-hydrodynamic circulation flow [31].

6 Fusion of drops or vesicles

Starting from the Taylor electro-hydrodynamic model for one leaky dielectric drop, the interaction of two leaky dielectric drops in a uniform DC electric field was calculated by Baygents et al. [29]. Assuming that the two drops are induced dipoles, dielectrophoresis favors translation of the drops toward one another. However, the electro-hydrodynamic circular flows may either act with or against the dielectrophoretic effect. Baygents et al. [29] showed that for sufficiently widely spaced drops, electro-hydrodynamic flows dominate over direct electrical interactions, and drop pairs may thus be pushed apart or pulled together depending on the directions of electro-hydrodynamic flow as described above. Sufficiently closely spaced drops almost always move together as a result of the electrical dipole interaction or elongation. Pairs of particle laden drops display the same effects as pure drops, and in this case it has been demonstrated by Rozynek et al. [14] (Fig. 10 and Fig. 11) how drop fusion may be used to produce so-called Janus or patchy colloidal capsules of various shapes.

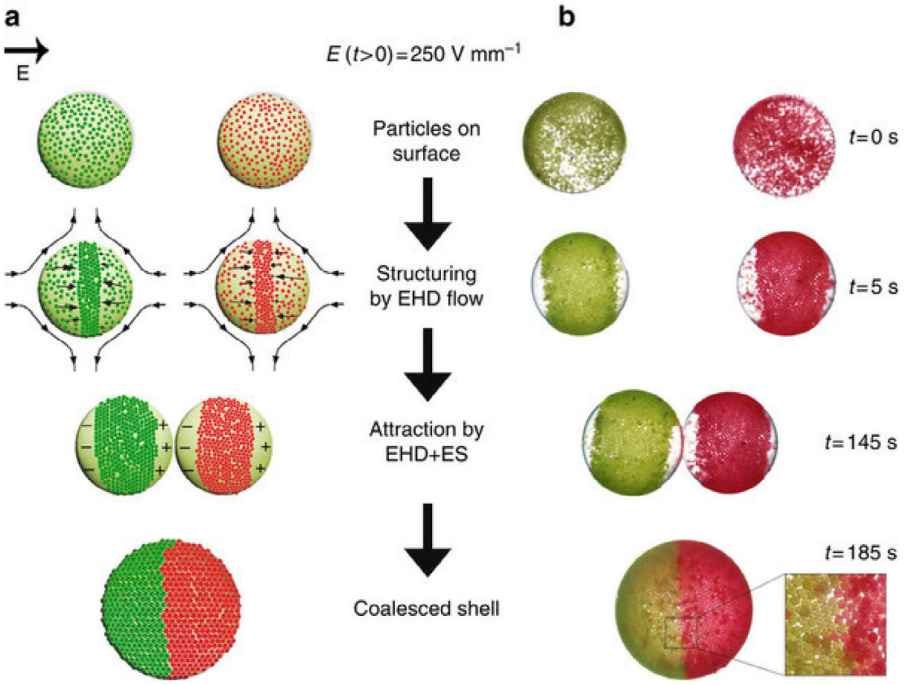

Fig. 10. The panels are taken from Rozynek et al. [14]. The left panels (a) are sketches, and the right panels (b) are experimental images, obtained by regular optical stereomicroscopy, of particle laden ∼mm diameter silicon oil drops embedded in a castor oil bath,. The panels display horizontal DC electric field alignment of, and induced electro-hydrodynamic formed ribbons in each of the particle (in this case 50 micrometer poly-ethylene (PE) red or green particles) laden drop. (0–5 s). This is, followed by electro-hydrodynamic (EHD) flow-induced, and electrostatic (ES) dipolar-induced, attraction of the two drops (5–145 s), and their subsequent electro-coalescence (185 s). Even if each of the two original particle laden drops are not fully covered by particles, the final coalesced drop can be fully and densely covered, as shown, due to reduction of the effective surface area of the coalesced drop compared to the sum of the two original drop surface areas. The drop fusion is significantly aided by the ribbon formation that brings the PE particles away from the drop electric poles. In this case, both original drops are covered with the same type of PE particles, only with different colors for visualization reasons, i.e. it is seen that the drops coalesce and form a densely packed Janus shell. Turning off the electric field does not induce observable particle movement within the shell, that is, the shell is stable, as the particles are arranged in a jammed, slightly disordered hexagonal structure as shown in the inset.

Figure 10 is reminiscent of vesicle fusion, as displayed in Fig. 12. Note here that pure vesicles are fluid capsules that cannot display jammed shapes as colloidal capsules can.

7 Higher electric DC fields

So far in this review, we have discussed particle structuring on drop interfaces exposed to moderately high DC electric fields, and we have explained the main effects caused by dielectrophoretic and electro-hydrodynamic mechanisms. If the electric field strength is increased, other phenomena may appear, as summarized by Ouriemi and Vlahovska [33], and as shown in Fig. 13. It is known that a dielectric drop suspended

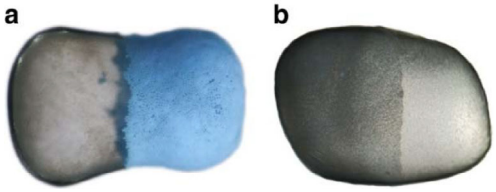

Fig. 11. The panels are taken from Rozynek et al. [14] showing microscope images of colloidal capsules produced in the same manner as the one displayed in Fig. 10. In this case however, the initial coverages of the two original drops are too large to accommodate a spherical Janus capsule product. Instead, since the particles are confined to the drop interface by capillary forces, the quasi two-dimensional particle system is jammed, and the fused shell is non-spherical. (a) Glass (500 nm) and blue polyethylene (20 micrometer) particles; (b) Polystyrene (1 micrometer) and clay mineral (∼ 1 micrometer) particles. These colloidal Janus capsules have asymmetric functionality in terms of permeability and conductivity.

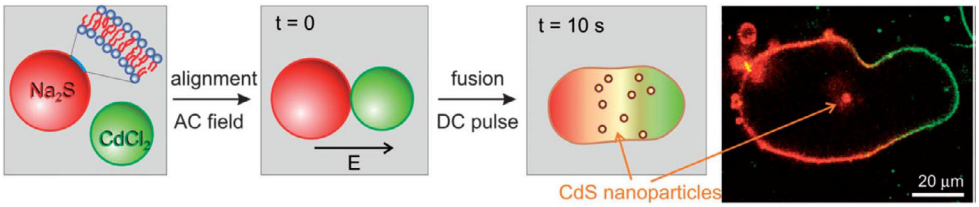

Fig. 12. The panels are taken from Yang et al. [32], and show a designed electro-fusion protocol for performing inorganic nanomaterial synthesis in giant vesicles. Vesicles containing Na_2S fluorescently labelled in red, and vesicles containing $CdCl_2$, labelled in green, are mixed in Na_2S-free and $CdCl_2$-free environment and subjected to an AC electric field to align them in the direction of the field and bring them close together. A DC electric pulse initiates the electro-fusion of the two vesicles and the reaction between Na_2S and $CdCl_2$ leads to formation of CdS nanoparticles encapsulated in the fused vesicle. The last snapshot is a confocal scan of a fused vesicle obtained by fusion of a vesicle loaded with Na_2S (red part of the fused vesicle) and a vesicle loaded with $CdCl_2$ (labelled in green). The fluorescence signal from the synthesized CdS nanoparticles in the vesicle interior is visible as indicated by the arrow.

in a conducting liquid and subjected to a uniform electric field deforms into an ellipsoid whose major axis is either perpendicular or tilted relative to the applied field, because of the so-called Quincke rotation effect [34,35]. Quincke rotation may occur when a particle or a drop with lower electric conductivity than that of the surrounding bath is exposed to a uniform DC electric field, thus inducing a free charge distribution build-up on the particle or drop surface, in effect making a dipole that point in opposite direction of the applied electric field. This dipole will try to turn around and align itself in the electric field, but rather than turning all the way around, it reaches a steady state of rotation due to the charges constantly fed to it by the leaky dielectric suspending liquid. Recently Ouriemi, and Vlahovska [33] studied particle laden leaky dielectric drops, and observed that at high surface coverage (90%), the electro-hydrodynamic flow is suppressed, oblate drop deformation is enhanced, and the threshold for the "Quincke tilt" is decreased compared to that of a particle-free drop.

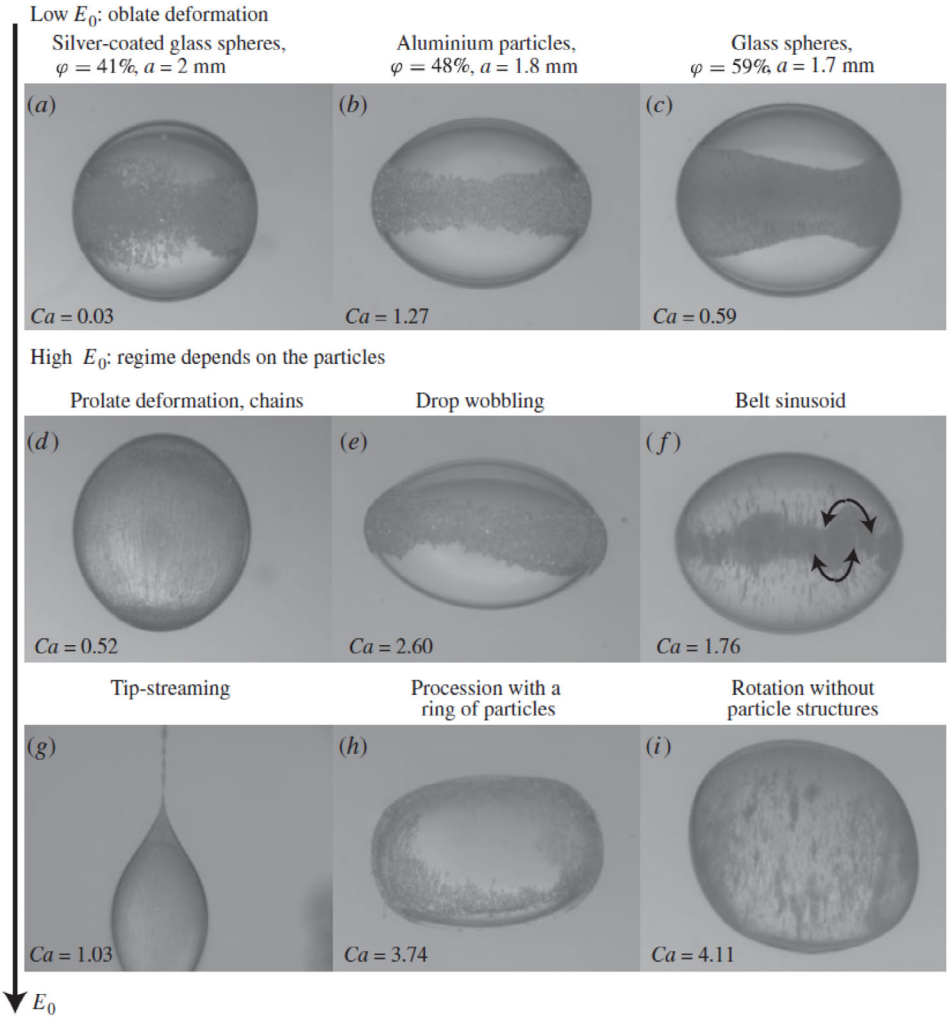

Fig. 13. The panels are taken from Ouriemi, and Vlahovska [33], who experimentally investigated the effect of particle laden leaky dielectric drops in a uniform DC electric field. They found that depending on the particle polarizability, coverage and the electrical field strength, particles assemble into various patterns (a)–(f) similar to those described by Ref. 8 and Ref. 14 earlier. Of particular interest are the observations (g)–(i) at high electric fields, including drop tip-streaming and rotations.

8 Summary and future directions

In this review, we have discussed one-drop or two-drop systems. Future work in this area may include studies of multiple-drop systems and emulsions [36], bulk mass production of structured capsules, and subsequently sintered or polymer cross-linked colloidosomes, for materials design. Figure 14 displays an initial study in this direction.

Another future direction is to study and make use of these effects at smaller drop sizes. This is feasible since the Taylor electro-hydrodynamic circulation flow periods are independent of the drop size [28], as is demonstrated in Fig. 15. Small drop systems could enable control of micro-emulsions for various purposes, or enable production of small functional capsules for chemical (including drug molecular) delivery purposes.

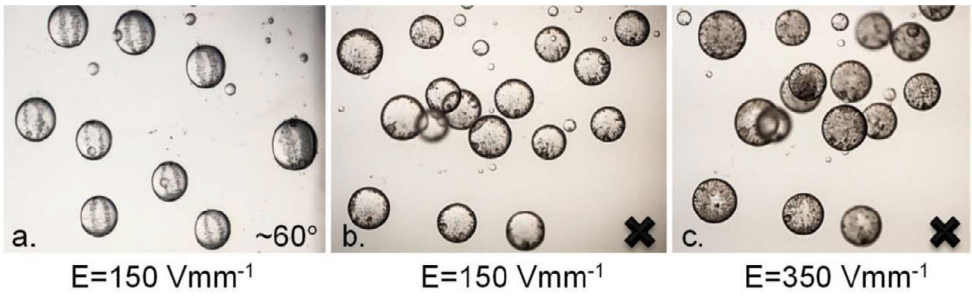

Fig. 14. Panels taken from Dommersnes et al. [8] showing active structuring of colloidal armor on multiple silicone oil drops embedded in castor oil (a) Simultaneously formed ribbons of clay particles at the surface of several drops viewed at an angle ∼60° with respect to the direction of electric field. Simultaneous opening (b), and closing (c), of multiple drops, similarly to the one-drop case in Fig. 8. The drop radii in these cases were in the range of 1 mm.

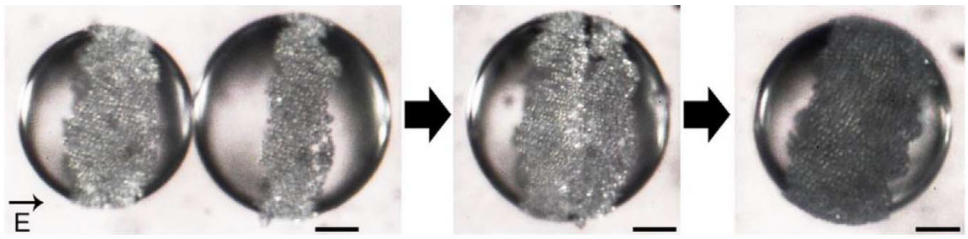

Fig. 15. Panels taken from Rozynek et al. [14] showing formation of colloidal ribbons from 1 micrometer particles at the surface of a small ∼ 50 micrometer diameter silicone oil droplet embedded in castor oil, produced by fusion of two particle laden original droplets. The electric fiied strength is 200 V/mm, and the process is equivalent to the one in Fig. 10 for larger drops.

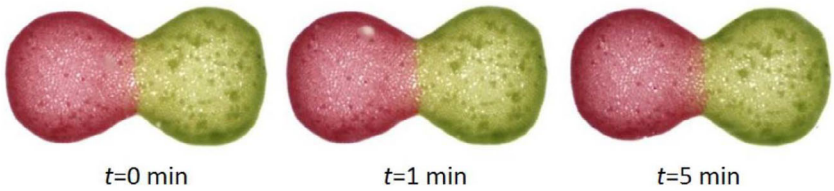

Fig. 16. Panels taken from Rozynek et al. [14] showing an example of a stable arrested capsule even after the electric field is turned off. This capsule which was produced as described in Fig. 11, demonstrate that arrested Janus/patchy capsules can be held stable during the time it takes to sinter or polymerize them for colloidosome production.

Finally, a future direction could be related to bulk mass production of functionalized Janus or patchy colloidosomes with designed shape. This adds possible shape functionality to the cases represented by Fig. 14 and Fig. 15, and Fig. 16 demonstrates that this is feasible.

We thank Z. Rozynek, A. Mikkelsen, R. Castberg, K. Kjerstad and K. Hersvik for their contributions to the experiments leading to Refs. 8, 9 and 14. We acknowledge financial support

from the Research Council of Norway (RCN) through a Petromaks2 ISP project (234125), and the Norwegian Centre for International Cooperation in Education (SIU) through an UTFORSK project (UTF-2014/10061). Finally, we thank the Centre for Advanced Study at the Norwegian Academy of Science and Letters for their generous support during the initial stages of this work.,

References

1. S.U. Pickering, J. Chem. Soc. **91**, 2001 (1907), doi: 10.1039/CT9079102001
2. C. Claire, Berton-Carabin, K. Schroën, Annual Rev. Food Sci. Technol. **6**, 263 (2015), doi: 10.1146/annurev-food-081114-110822
3. J. Tang, P.J. Quinlan, K. Chiu, Soft Matter **11**, 3512 (2015), doi: 10.1039/C5SM00247H
4. S. Lam, K.P. Velikov, O.D. Velev, Current Opinion Coll. Interface Sci. **19**, 490 (2014)
5. B. Neirinck, J. Fransaer, O. Van der Biest, J. Vleugels, Adv. Eng. Mater. **9**, 57 (2007), doi: 10.1002/adem.200600191
6. S. Fujii, Y. Eguchi, Y. Nakamura, RSC Adv. **4**, 32534 (2014), doi: 10.1039/c4ra04409f
7. P.S. Clegg, J.W. Tavacoli, P.J. Wilde, Soft Matter (Review Article) **12**, 998 (2016), doi: 10.1039/C5SM01663K
8. P. Dommersnes, Z. Rozynek, A. Mikkelsen, R. Castberg, K. Kjerstad, K. Hersvik, J.O. Fossum, Nat. Comm. **4**, 2066 (2013), doi: 10.1038/ncomms3066
9. Z. Rozynek, P. Dommersnes, A. Mikkelsen, L. Michels, J.O. Fossum, Eur. Phys. J. Special Topics **223**, 1859 (2014), doi: 10.1140/epjst/e2014-02231-x
10. A.D. Dinsmore, M.F. Hsu, M.G. Nikolaides, M. Marquez, A.R. Bausch, D.A. Weitz, Science **298**, 1006 (2002)
11. R. Fantoni, J.W.O. Salari, B. Klumperman, Phys. Rev. E. **85**, 061404 (2012), doi: 10.1103/PhysRevE.85.061404
12. S. Nudurupati, M. Janjua, N. Aubry, P. Singh, Electrophoresis **29**, 1164 (2008)
13. E. Amah, K. Shah, I. Fischer, P. Singh, Soft Matter, 2016, Adv. Article, doi: 10.1039/C5SM02195B
14. Z. Rozynek, A. Mikkelsen, P. Dommersnes, J. Otto Fossum, Nat. Comm. **5**, 3945 (2014), doi: 10.1038/ncomms4945
15. P. Sheng, W. Wen, **44**, 143 (2012), doi: 10.1146/annurev-fluid-120710-101024
16. J.O. Fossum, Y. Meheust, K.P.S. Parmar, et al., Europhysics Lett. **74**, 438 (2006)
17. E. Amah, K. Shah, I. Fischer, P. Singh, Soft Matter, 2016, Adv. Article, doi: 10.1039/C5SM02195B
18. S. Nudurupati, M. Janjua, P. Singh, et al., Phys. Rev. E. **80**, 010402 (2009)
19. K. Hwang, P. Singh, N. Aubry, Electrophoresis **31**, 850 (2010)
20. W. He, N. Şenbil, A.D. Dinsmore, Soft Matter **11**, 5087 (2015), doi: 10.1039/C5SM00245A
21. R. Dimova, N. Bezlyepkina, M.D. Jordö, R.L. Knorr, K.A. Riske, M. Staykova, P.M. Vlahovska, T. Yamamoto, P. Yang, R. Lipowsky, Soft Matter **5**, 3201 (2009)
22. A. Walther, A.H.E. Müller, Chem. Rev. **113**, 5194 (2013), doi: 10.1021/cr300089t
23. A.B. Pawar, I. Kretzschmar, Macromolecular Rapid Communications, Special Issue: Multifunctional Micro- and Nanoparticles **31**, 150 (2010), doi: 10.1002/marc.200900614
24. S. Nudurupati, M. Janjua, P. Singh, N. Aubry, ASME Proceedings: Heat Transfer, Fluid Flows, and Thermal Systems **10**, 159 (2009)
25. Y. Méheust, K. Parmar, B. Schjelderupsen, J.O. Fossum, J. Rheol **55**, 809 (2011)
26. G. Taylor, Proc. Roy. Soc. Lond. A **291**, 159 (1966)
27. R.S. Allan, S.G. Mason, P Proc. Roy. Soc. Lond. A **267**, 45 (1962)
28. D.A. Saville, Annu. Rev. Fluid Mech. **29**, 27 (1997)
29. J.C. Baygents, N.J. Rivette, H.A. Stone, J. Fluid Mech. **368**, 359 (1998)
30. M.L. Yarmush, A. Golberg, G. Serša, T. Kotnik, D. Miklavčič, Ann. Rev. Biomedical Eng. **16**, 295 (2014), doi: 10.1146/annurev-bioeng-071813-104622
31. S. Lecuyer, W.D. Ristenpart, O. Vincent, H.A. Stone, Appl. Phys. Lett. **92**, 104105 (2008)

32. P. Yang, R. Lipowsky, R. Dimova, Small **5**, 2033 (2009), doi: 10.1002/smll.200900560
33. M. Ouriemi P.M. Vlahovska, J. Fluid Mechan. **751**, 106 (2014), doi: 10.1017/jfm.2014.289
34. G. Quincke, Annalen der Physik **295**, 417 (1896), doi: 10.1002/andp.18962951102
35. D. Das, D. Saintillan, Phys. Rev. E **87**, 043014 (2013)
36. L.A. Fielding, S.P. Armesa, J. Mater. Chem. **22**, 11235 (2012), doi: 10.1039/C2JM31433A